

Preparation and Characterization of Poly(vinyl alcohol)-Modified Red Mud Composite Materials

A. H. Bhat, A. K. Banthia

Materials Science Centre, Indian Institute of Technology Kharagpur, Kharagpur 721302, India

Received 28 April 2006; accepted 17 July 2006

DOI 10.1002/app.25180

Published online in Wiley InterScience (www.interscience.wiley.com).

ABSTRACT: A series of polymer–acid-modified red mud composite (PRM) materials that consist of poly(vinyl alcohol) (PVA) and layered Red mud (RM) are prepared by effectively dispersing organic PVA matrix into the inorganic layers of modified RM via a conventional solvent casting technique. The as-synthesized PRM materials are typically characterized by Fourier transformation infrared (FTIR) spectroscopy and wide-angle X-ray diffraction. The morphological image of as-synthesized materials is studied by scanning electron microscopy (SEM) and optical micro-

scope (OM). Effects of the material composition on the thermal stability and optical clarity of PVA along with a series of PRM materials freestanding film are also studied by thermogravimetric analysis (TGA), differential scanning calorimetry (DSC) and UV–vis transmission spectra, respectively. © 2006 Wiley Periodicals, Inc. *J Appl Polym Sci* 103: 238–243, 2007

Key words: polymer–acid-modified red mud; poly(vinyl alcohol); acid-modified red mud

INTRODUCTION

Red mud is a waste obtained from the aluminum industry and has been accumulating at a rate of 30 million ton annually throughout the world. Under normal conditions when 1 ton of alumina is produced from bauxite, an equal amount of red mud is generated as a waste. The disposal of red mud is associated with space/real estate near industry, cost of disposal, and pollution, which are now crucial factors. Therefore, the exploitations of these by-products are a growing technological aspect of basic industries and the environment. A further aspect is their reuse as starting materials for other products.^{1–2} Red mud has been suggested as filler for polymer reinforcement or as a cheap adsorbent for removal of toxic metals or an acid by several researchers. Chand and Hashmi^{3–4} tried to improve the mechanical properties and abrasive wear properties of polymer blend filled with red mud. Pradhan et al.⁵ had reported that activated red mud as a good adsorbent was used for adsorption of phosphate or chromium. In addition, the mechanical and thermal properties of polymers are generally improved by the addition of inorganic fillers. The challenges in this area of high-performance organic–inorganic hybrid materials are to obtain significant improvements in the interfacial adhesion between the polymer matrix and the reinforcing material since the organic matrix is rela-

tively incompatible with the inorganic phase. Generally, a better interfacial bonding will impart better properties to a polymer composite such as high modulus, strength, and stiffness.^{6–7} This reinforcement of polymer filled with inorganic material is largely dependent on the physical interfacial phenomenon between the filler and matrix. This can be determining the degree of adhesion by physical interaction, such as active functional groups, hydrogen bonding, Lewis acid–base interactions, surface energy, and crystallite faces of filler surface at the interface.^{8–9} To increase physical interaction, various surface treatment techniques are applied, such as oxidation in acid solutions,¹⁰ dry oxidation in oxygen,¹¹ anodic oxidation,^{12–13} and plasma treatments.¹⁴ Surface modification leads to development of surface functional activity on a filler surface, resulting in modification to achieve good interfacial adhesion between the reinforcement and the matrix. In this paper, red mud is modified by treating it with boric acid to increase its interfacial adhesion with the polymer matrix.

Composite materials consisting of inorganic layers of acid-modified red mud and organic polymers have evoked intense research interests nowadays because their unique characteristics create many potentially commercial applications. PRM are reported to promote the thermal,¹⁵ mechanical,¹⁶ molecular barrier,¹⁷ flame retardant,¹⁸ and corrosion protection properties^{19–21} of polymers at low clay loading. Recently, polymer–clay materials that consist of PVA and layered materials are found to display novel properties, which can be observed from two dissimilar chemical components combining at the molecular level. There

Correspondence to: A. H. Bhat (aamir_bhat@rediffmail.com).

TABLE I
Sample Designation

Sample index	% Loading of modified red mud
PVA	0
SP1	0.5
SP2	1
SP3	1.5
SP4	2
SP5	3
SP6	4
SP7	5
SP8	7
SP9	10

are several publications associated with the preparation and properties of PVA–Clay composite materials. However, preparation and characteristic studies of PVA–red mud composite materials have not been reported. In this study, we prepare a series of PRM materials by effectively dispersing the inorganic layers of acid-modified red mud in organic PVA matrix via a conventional solvent casting technique. For the hydrophilic films intercalation or exfoliation can be achieved by directly mixing the red mud with the polymer above its softening temperature. The as-synthesized PRM materials are characterized by Fourier transformation infrared (FTIR) spectroscopy and wide-angle X-ray diffraction (XRD). The morphological images of as-synthesized materials are also studied by SEM and OM. Effects of the material composition on the thermal stability, optical clarity of PVA along with a series of PRM materials in the form of free-

standing film, are also studied by TGA, DSC, and UV–vis transmission spectra, respectively.

EXPERIMENTAL

Chemicals and instrumentations

PVA (M_w : 125,000 and degree of hydrolysis approx. 88%) was obtained from S.D. fine-Chemicals Ltd. (Mumbai, India). Distill water was used throughout the study. Higher molecular weights produce a more a “stiffer” slime while lower molecular weights produce amore fluid, “slimier” slime.

Red mud (RM), a waste material from a Bayer process (~35–40% per ton of bauxite-treated using the Bayer process ends up as red mud waste) was provided by R & D Laboratory of NALCO (Damanjodi, Orissa, India), was used as an inorganic filler. It is bright red in color, and magnetic in nature. This iron-containing powdered clay material is readily distributed in water.

Attenuated Total Reflection (ATR) spectra in the range of 4000–400 cm^{-1} of the PRM films were measured with FTIR Spectroscope (NEXUS-870, Thermo Nicolet) running Omnic software, and a uniform resolution of 2 cm^{-1} was maintained in all cases. The nature of the PRM films was investigated by means of X-ray diffraction (XRD-PW 1710 diffractometer unit, Philips) using Co K α radiation generated at 40 kV and 20 mA at a scan rate of 3° min^{-1} ; the range of diffraction angle 2 θ was 10–60°.

A NETZSCH DSC-200 PC was used for studying the melting and crystallization behavior of the PRM

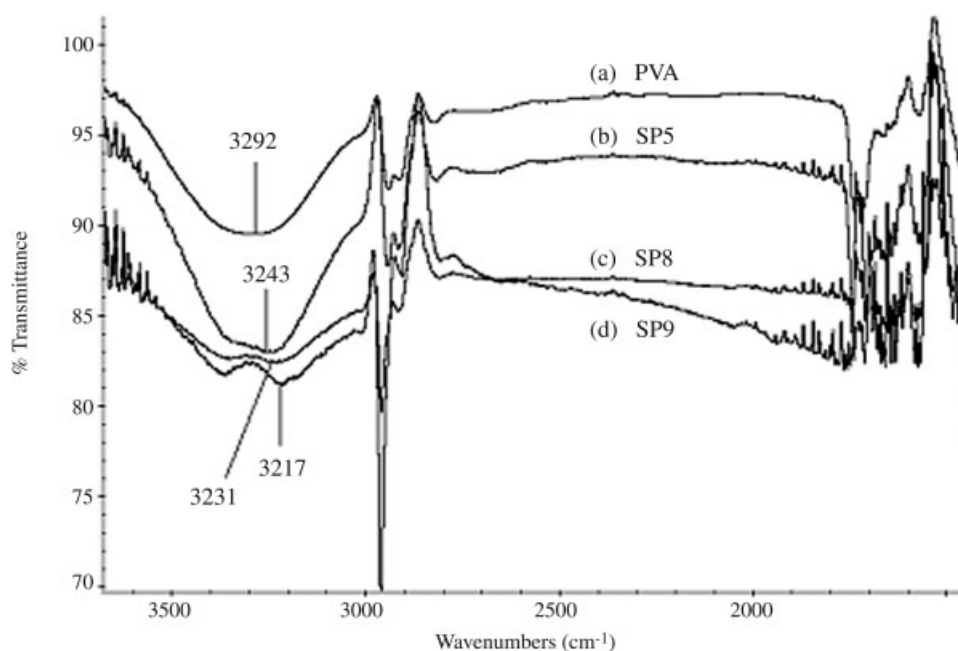


Figure 1 FTIR Spectra of (a) PVA (b) SP5 PRM (c) SP8 PRM, and (d) SP9 PRM films.

films. The melting studies were performed in the 30–300°C range under N₂ flow at the programmed heating rate of 10°C min⁻¹.

Thermal analysis was carried out by using Perkin–Elmer Instrument (Pyris Diamond DTA/TG), under atmosphere, at a heating rate of 10°C min⁻¹.

A scanning electron microscope (SEM) (JOEL, JSM 5800) was used to analyze the morphological images of the PRM films.

Morphological images of PVA and PRM films were also studied by LEICA MPS 30 optical microscope.

UV–vis transmission spectra of PVA along with a series of PRM films were recorded by using DH-2000 Mikropack UV–vis spectrometer.

Preparation of acid-modified red mud

The 5 g raw red mud is first washed with distilled water two to three times and then dried in an oven.

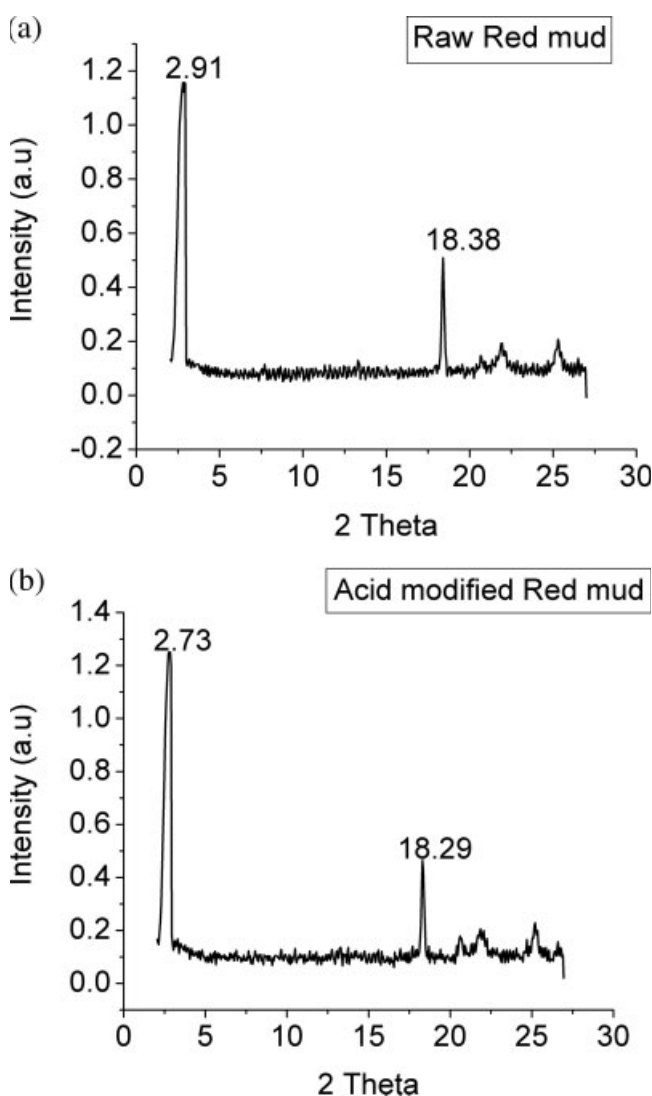


Figure 2 XRD pattern of (a) Raw red mud (b) Acid-modified red mud.

TABLE II
Crystallite Size of Red Mud Calculated from Figure 2(a)

2θ	<i>D</i> (nm)	<i>⟨D⟩</i> (nm)
2.91	44.28	66.965
18.38	89.65	

when the red mud is completely dried, it is being treated with a 5M solution of boric acid for 24 h. Then it is being filtered, dried, weighed, and grinded to get its powdered form. The weight of the red mud is increased by 24%. The powder is then sieved through 53 micron mesh to remove the larger particles. The powder thus obtained is fine and is acidically modified.

Preparation of PVA-Red Mud composite materials

PVA solution was prepared at a concentration of 10 wt % by dissolving dried powdered PVA in distilled water at a temperature of 100°C under continuous stirring. PRM films were made by mixing different loading percentage of acid-modified red mud with respect to calculated amount of PVA. The samples were designated as shown in Table I.

RESULTS AND DISCUSSIONS

PVA has been used for many industrial applications such as paper processing, textile sizing and finishing, adhesives and binders, dispersant and molded products.

On the other hand, red mud is produced during the digestion of bauxite with sodium hydroxide. It generally exits the process stream as highly alkaline slurry (pH 10–12.5) at approximately 15–30% solids,²² from where it is pumped away for appropriate disposal. Red mud is composed primarily of fine particles of silica, aluminum, iron, calcium, and titanium oxides and hydroxides (along with other minor components), with the iron impurities responsible for brick red color of the mud. Red mud thus has a complex chemical composition (largely dependent on the bauxite source) and, due to its high calcium (CaCO₃/3CaO · Al₂O₃ 6H₂O) and NaOH content, is relatively toxic and can pose a serious pollution hazard. The composition of the PRM materials is varied from 0 to 10 wt % of clay with respect to the PVA content.

TABLE III
Crystallite Size Calculated from Figure 2(b)

2θ	<i>D</i> (nm)	<i>⟨D⟩</i> (nm)
2.73	49.05	60.36
18.29	71.71	

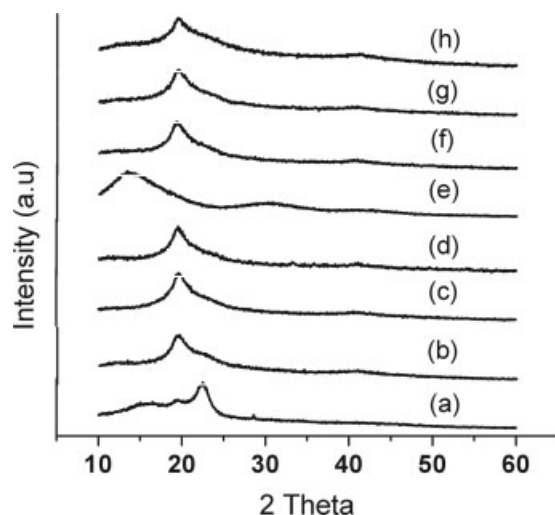


Figure 3 Wide-angle powder XRD patterns of (a) PVA, (b) SP1 PRM, (c) SP3, (d) SP4, (e) SP5, (f) SP6, (g) SP7, and (h) SP9.

Characterization

The representative FTIR spectra of the pure PVA and PRM materials are shown in Figure 1. The characteristic vibration bands of PVA are shown at 3292 cm^{-1} (OH), 2945 cm^{-1} ($-\text{CH}_3$), 2913 cm^{-1} (CH_2), 1730 cm^{-1} ($\text{O}=\text{C}$), 1242 cm^{-1} ($\text{C}-\text{O}-\text{C}$), and 1422 cm^{-1} ($\text{O}-\text{H}$, C—H Bending) and those of PRM are shown at $3217\text{--}3243\text{ cm}^{-1}$ ($\text{O}-\text{H}$), $1243\text{--}1261\text{ cm}^{-1}$ ($\text{Si}-\text{O}$), and $1320\text{--}1372\text{ cm}^{-1}$ ($\text{B}-\text{O}$). A decrease in the absorbance of the peak at $3217\text{--}3292\text{ cm}^{-1}$ in the PRM films arises because of the disappearance of the hydroxyl groups upon crosslinking reaction with the boric acid.

Wide angle X-ray diffraction

Wide angle X-ray diffraction studies have been performed on both the modified and unmodified red

TABLE IV
Variation of Crystallinity with Filler Content

Sample name	% Crystallinity
PVA	10.69
SP1	9.81
SP3	8.32
SP4	6.99
SP5	3.90
SP6	4.89
SP7	4.75
SP9	5.87

mud. The result obtained from Figure 2(b) clearly demonstrates the presence of a predominant peak in the vicinity of 2.73° . Applying Debye–Scherer Equation [eq. (1)] to calculate the crystallite size we have,

$$D = \frac{\Phi\lambda}{\beta \cos \theta} \quad (1)$$

where, β is the breadth of the peak at half intensity.

Φ is a constant depending upon the source of X-ray.

X-ray was generated using Cobalt source with characteristic monochromatic wavelength of 1.78 \AA . Thus, the crystallite size for the above system using eq. (1) is given by

$$D = \frac{(1.78 \times 10^{-10}) \times (1.79 \times 10^{-10})}{(0.781 \times \cos 1.365)}$$

Hence, the calculated D value is 49.05 nm (Tables II and III). The wide angle diffraction of PRM films is shown in Figure 3. There is decrease in the crystallinity of PRM films as the loading percentage of modified red mud increases and is minimum for SP5 due to greater extent of exfoliation. This is shown by the Table IV below. The changing of crystalline behavior can be further evi-

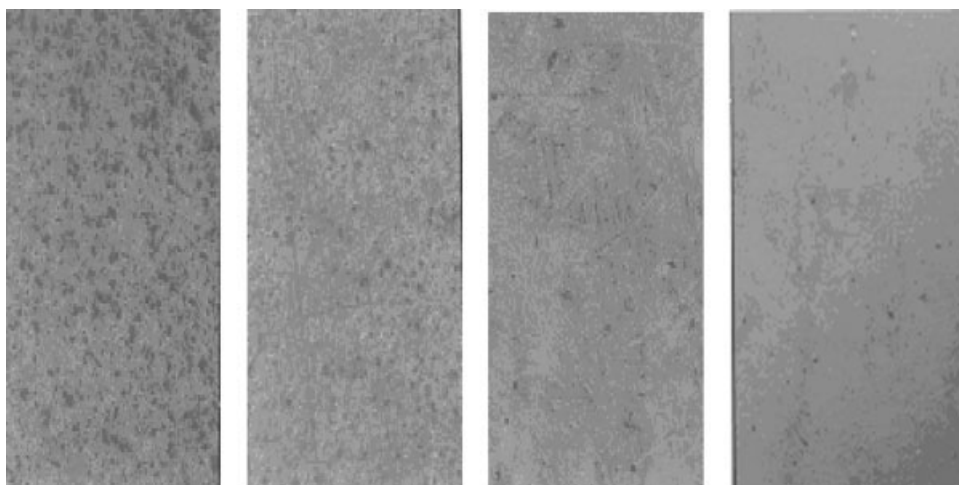


Figure 4 Optical microscopic images of (a) PVA PRM, (b) SP1 PRM, (c) SP4 PRM, and (d) SP5 PRM.

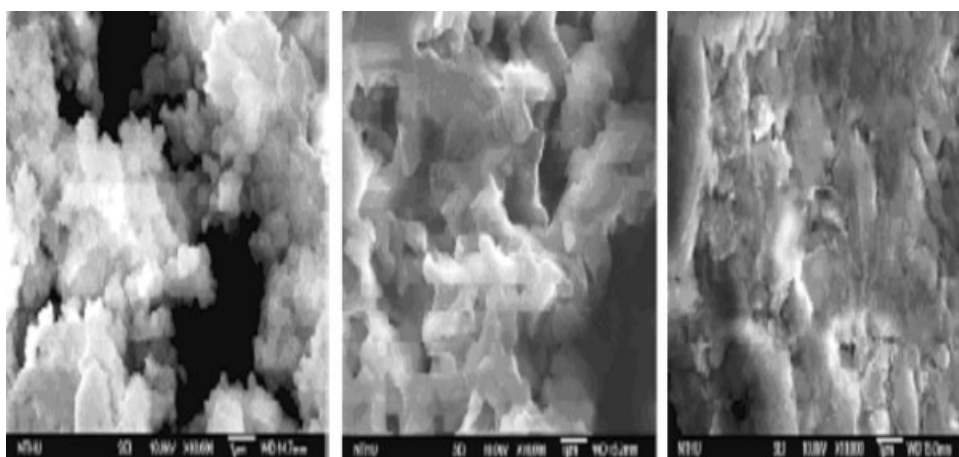


Figure 5 SEM micrographs of (a) PVA, (b) SP4 PRM, and (c) SP5 PRM.

denced by the studies of the morphological image of as-synthesized materials by SEM and OM. Individual silicate layers, along with two, three, and four layer stacks, are exfoliating in the PVA matrix. In addition, some larger intercalated tactoids could also be identified.

Morphological image studies

The morphological image of as-synthesized materials is studied by SEM and OM. The SEM images in Figure 5 show that the morphology of PRM films becomes much smooth than pure PVA. The granules shape of PVA indicates some crystalline behavior occurring in pure polymer. The incorporation of red mud seems to destroy the orientation of crystalline polymer and to convert the polymer morphology approaching to amorphous state. This observation is also conformed by OM, as shown in Figure 4. The SP5 PRM shows much smooth morphology that is different to crystalli-

tes of PVA observation. This result is consistent with the wide-angle powder XRD patterns as described previously.

Thermal properties of PRM films

Figure 6 shows a typical TGA thermogram of weight loss as a function of temperature for PRM materials along with PVA, as measured under nitrogen atmosphere. In general, major weight losses are observed in the range of 200–500°C for PVA and PRM films, which may be correspondent to the structural decomposition of the polymers. Evidently, the thermal decomposition of those PRM materials shift slightly towards the higher temperature range than that of PVA, which confirms the enhancement of thermal stability of intercalated polymer.²³ After, 600°C, the curve all became flat and mainly the inorganic residue (i.e., Al_2O_3 , MgO , and SiO_2) remained. DSC traces of PVA and

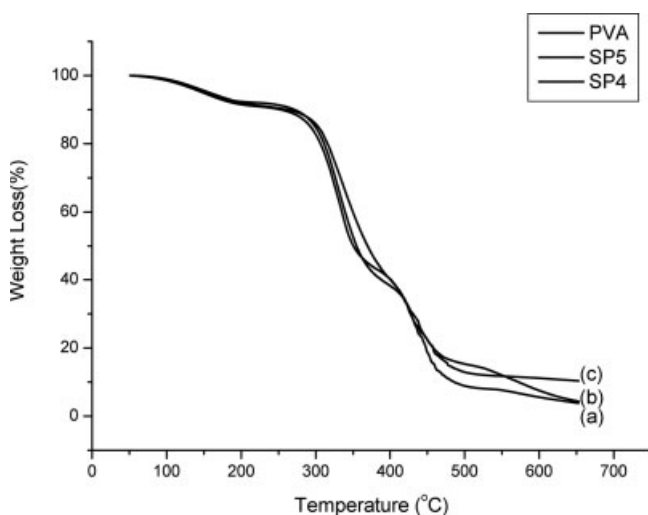


Figure 6 Thermograms of (a) PVA, (b) SP4, and (c) SP5 PRM film.

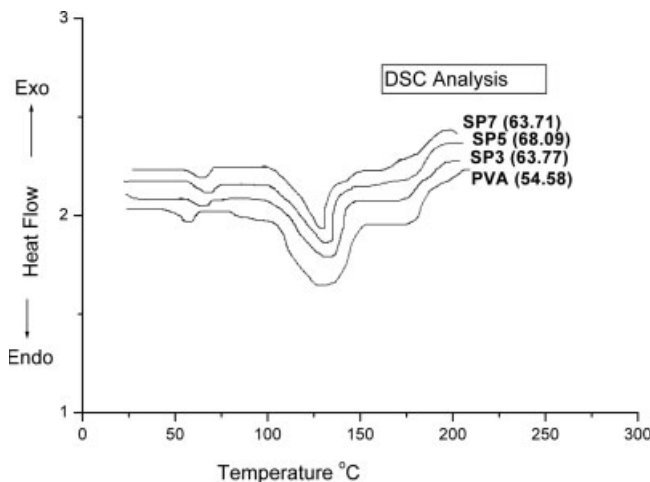


Figure 7 DSC thermograms of (a) PVA, (b) SP4, (c) SP6, and (d) SP5.

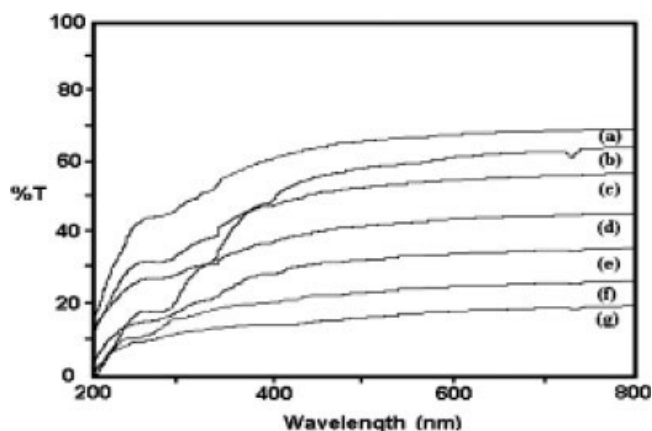


Figure 8 UV-visible transmission spectra of (a) PVA, (b) SP1, (c) SP4, (d) SP5, (e) SP7, (f) SP8, and (g) SP9 PRM membrane.

PRM materials are shown in Figure 7. PVA exhibits an endotherm at 54.58°C corresponding to the glass transition temperature (T_g) of PVA.²⁴ All the PRM materials are found to have a high T_g compared with the bulk PVA. This is tentatively attributed to the confinement of the intercalated polymer chains within the clay galleries that prevents the segmental motions of the polymer chains.

Optical clarity of membrane

The membranes of bulk PVA and PRM materials used for optical property measurements are prepared to have film thickness of 20 mm. Figure 8(a–g) shows that the UV-vis transmission spectra of pure PVA and PRM membranes. The transmission spectra of pure PVA and PRM membranes in the visible light regions (200–800 nm) are slightly affected by the presence of the low red mud loading in the PRM membranes. However, the spectra of as-prepared membrane at higher red mud loading (e.g. SP5) exhibits lower optical clarity, reflecting that there is strong scattering of red mud resulting in lower transparency of the UV-vis light.

CONCLUDING REMARKS

A series of nanocomposite materials that consist of PVA and layered Red mud are prepared by effectively dispersing the inorganic nanolayers of red mud in organic PVA matrix via a solvent intercalation technique. As-synthesized PRM materials are characterized by FTIR spectroscopy and XRD. The morpholo-

gies of as-synthesized PRM materials are studied through SEM and OM. The crystalline morphology of PVA approaches to amorphous state as the red mud loading increases. This is consistent with the observation of XRD patterns, in which an intense peak appearing at $2\theta = 22.55^\circ$ for PVA is decreased when the loading of red mud increases in PRM materials. Thermal stability and optical clarity of PVA as well as a series of PRM materials, in the form of membranes, are also investigated by TGA, DSC, and UV-vis transmission spectra, respectively. The incorporation of nanolayers of red mud in PVA matrix results in an increase in thermal decomposition temperature and glass transition temperature based on TGA and DSC respectively. The UV-vis transmission spectra exhibit lower transparency when red mud content increases and shows least optical clarity in case of SP5 film.

References

- Grjotheim, K.; Welch, B. J. *Aluminium Smelter Technology: A Pure and Applied Approach*, 2nd ed.; Verlag: Dusseldorf, 1998.
- Kasliwal, P.; Sai, P. S. T. *Hydrometallurgy* 1999, 53, 73.
- Chand, N.; Hashmi, S. A. R. *J Sci Ind Res* 1999, 58, 795.
- Chand, N.; Hashmi, S. A. R. *Bull Mater Sci* 1999, 22, 801.
- Pradhan, J.; Das, S. N.; Thakur, R. S. *J Colloid Interface Sci* 1999, 217, 137.
- Agag, T.; Koga, T.; Takeichi, T. *Polymer* 2001, 42, 3399.
- Jang, B. Z. *Compos Sci Technol* 1992, 44, 333.
- Park, S. J.; Kim, J. S. *J Colloid Interface Sci* 2000, 232, 311.
- Park, S. J.; Cho, M. S. *Carbon* 2000, 38, 1053.
- Donnet, J. B.; Bansal, R. C. *Carbon Fibers*, 2nd ed.; Dekker: New York, 1990.
- Yuan, L. T.; Shyu, S. S.; Lai, J. Y. *J Appl Polym Sci* 1991, 42, 2525.
- Ishikawa, Y.; Matsumoto, Y. *Electrochem Acta* 2001, 46, 2819.
- Park, S. J.; Kim, M. H. *J Mater Sci* 2000, 35, 1901.
- Dilsiz, N.; Ebert, E.; Weisweiler, W.; Akovali, G. *J Colloid Interface Sci* 1995, 170, 241.
- Lan, T.; Kaviratna, P. D.; Pinnavaia, T. *J Chem. Mater* 1994, 6, 573.
- Tyan, H. L.; Liu, Y. C.; Wei, K. H. *Chem Mater* 1999, 11, 1942.
- Wang, Z.; Pinnavaia, T. *J Chem Mater* 1998, 10, 3769.
- Gilman, J. W.; Jackson, C. L.; Morgan, A. B.; Hayyis, R., Jr.; Manias, E.; Giannelis, E. P.; Wuthenow, M.; Hilton, D.; Philips, S. H. *Chem Mater* 2000, 12, 1866.
- Yeh, J. M.; Liou, S. J.; Lai, C. Y.; Wu, P. C.; Tsai, T. Y. *Chem Mater* 2001, 13, 1131.
- Yeh, J. M.; Chen, C. L.; Chen, Y. C.; Ma, C. Y.; Lee, K. R.; Wei, Y.; Li, S. *Polymer* 2002, 43, 2729.
- Yeh, J. M.; Liou, S. J.; Lin, C. Y.; Cheng, C. Y.; Chang, Y. W.; Lee, K. R. *Chem Mater* 2002, 14, 154.
- Zouboulis, A. I.; Kydros, K. A. *J Chem. Technol Biotechnol* 1993, 58, 95.
- Lee, D. C.; Jang, L. W. *J Appl Polym Sci* 1996, 61, 1117.
- Strawhecker, K. E.; Manias, E. *Chem Mater* 2000, 12, 2943.